Published in final edited form as:
J Immunol. 2014 June 15; 192(12): 5476–5480. doi:10.4049/jimmunol.1400499.

RIP1 kinase activity is dispensable for normal development but is a key regulator of inflammation in SHARPIN-deficient mice

Scott B. Berger[*], **Viera Kasparcova**[*], **Sandy Hoffman**[*], **Barb Swift**[*], **Lauren Dare**[*], **Michelle Schaeffer**[*], **Carol Capriotti**[*], **Michael Cook**[*], **Joshua Finger**[*], **Angela Hughes-Earle**[†], **Philip A. Harris**[*], **William J. Kaiser**[‡], **Edward S. Mocarski**[‡], **John Bertin**[*], and **Peter J. Gough**[*]

[*]Pattern Recognition Receptor Discovery Performance Unit, Immuno-inflammation Therapeutic Area

[†]Safety Assessment, Platform Technology Sciences; GlaxoSmithKline, Collegeville, PA, USA

[‡]Department of Microbiology and Immunology, Emory Vaccine Center, Emory University School of Medicine, Atlanta, Georgia, USA

Abstract

RIP1 kinase is a key regulator of TNF-induced NFκB activation, apoptosis and necroptosis through its kinase and scaffolding activities. Dissecting the balance of RIP1 kinase activity and scaffolding function *in vivo* during development and TNF-dependent inflammation has been hampered by the perinatal lethality of RIP1-deficient mice. Here we generated RIP1 kinase-dead (*Ripk1*^{K45A}) mice and showed they are viable and healthy, indicating that kinase activity of RIP1, but not its scaffolding function, is dispensable for viability and homeostasis. After validating that the *Ripk1*^{K45A} mice were specifically protected against necroptotic stimuli *in vitro* and *in vivo*, we crossed these mice to SHARPIN-deficient *cpdm* mice, which develop severe skin and multi-organ inflammation that has been hypothesized to be mediated by TNF-dependent apoptosis and/or necroptosis. Remarkably, crossing *Ripk1*^{K45A} mice to the *cpdm* strain protected against all *cpdm*-related pathology. Together, these data suggest that RIP1 kinase represents an attractive therapeutic target for TNF-driven inflammatory diseases.

Introduction

TNF is a pleiotropic cytokine that was first described as causing necrosis in tumors (1), but has since been recognized as a major driver of inflammation and human disease pathogenesis (2). TNF binding to its receptor, TNF receptor 1 (TNFR1), results in one of three distinct cellular fates, NFκB activation, apoptosis or necrosis. The serine/threonine kinase receptor-interacting protein 1 (RIP1) serves as a key decision checkpoint for these different fates through its function as a scaffolding protein and its kinase activity (3). Under conditions where RIP1 is highly ubiquitinated, TNFR1 engagement activates NFκB to promote gene transcription and cell survival. In situations where RIP1 is deubiquitinated, TNF initiates one of two programmed cell death pathways; apoptosis, or the recently

Correspondence to: Peter J. Gough, GlaxoSmithKline, Pattern Recognition Receptor DPU, 1250 South Collegeville Rd., Collegeville, PA 19426, Phone: 610-917-6099, peter.j.gough@gsk.com.

discovered necroptosis pathway that requires conditions of caspase inhibition (4). *In vitro* experiments using the RIP1 kinase inhibitor Necrostatin-1 (Nec-1) have shown that RIP1 kinase activity is critical for TNF-induced necroptosis, but appears dispensable for NFκB activation and apoptosis (5). However, at present, the exact contribution of RIP1 kinase activity to viability, homeostasis and inflammation *in vivo* is unknown as RIP1-deficient mice die shortly after birth (6), and current pharmacological tools are unsuitable for chronic RIP1 inhibition (5).

TNFR1-mediated activation of NFκB is dependent upon the ubiquitination of RIP1 by the linear ubiquitin chain assembly complex (LUBAC), comprised of the enzymes HOIL, HOIP and SHARPIN (7). Cells lacking LUBAC function through deficiency of SHARPIN show no detectable NFκB activation following TNF stimulation, but are highly sensitive to TNF-induced apoptosis and RIP1-kinase dependent necroptosis (8). SHARPIN-deficient, chronic proliferative dermatitis (*cpdm*), mice develop a TNF-dependent multi-organ inflammatory pathology including a severe dermatitis (9). The *in vitro* data suggest that development of inflammation in *cpdm* mice is likely mediated by excessive TNF-dependent apoptosis and/or necroptosis. Both apoptosis and necroptosis have been implicated in driving inflammation in disease settings, and therefore the precise contributions of these cell death pathways in the pathogenesis of disease in the *cpdm* mouse remains unknown.

In this article, we generated RIP1 kinase-dead (*Ripk1*^{K45A}) mice and showed that they are viable and healthy. *Ripk1*^{K45A} mice showed a selective defect in TNF-induced necroptosis *in vitro*, and were resistant to a lethal TNF-dependent shock *in vivo*. Crossing *Ripk1*^{K45A} mice with the *cpdm* line completely rescued the skin and tissue inflammatory pathology, highlighting the inflammatory potential of RIP1 kinase-dependent necroptosis and signaling in TNF-driven diseases.

Materials and Methods

Mice

RIP1 kinase-dead knock-in (*Ripk1*^{K45A}) mice were generated as described in Figure 1A. Additional information is available upon request. *cpdm* mice were purchased from Jackson Laboratories. All animal procedures were conducted in an Association for Assessment and Accreditation of Laboratory Animal Care (AAALAC)-accredited facility at GlaxoSmithKline in accordance with the GlaxoSmithKline Policy on the Care, Welfare, and Treatment of Laboratory Animals, and were reviewed and approved by the Institutional Animal Care and Use Committee (IACUC) at GlaxoSmithKline.

Preparation of bone marrow derived and peritoneal macrophages

Bone marrow-derived macrophages (BMDM) were prepared from bone marrow by differentiation with 10ng/ml M-CSF (R&D Systems). Thioglycolate-elicited peritoneal macrophages (TM) were obtained from mice that had been injected with 1.5ml 4% thioglycolate (Difco).

Cytokine and serum IgM analysis and Western blotting

Cytokines were measured using the Mouse Proinflammatory 7-Plex Ultra-Sensitive kit (Meso Scale Discovery). Serum IgM was measure by ELISA (eBioscience). To examine protein expression in tissues, lysates were run on SDS-PAGE and blotted onto nitrocellulose membranes (Invitrogen). Blots were probed for β-actin (Sigma), RIP1 (BD Biosciences) and RIP3 (Imgenex). For TNF activation experiments, BMDM were treated with 50ng/ml of TNF (R&D systems) and lysates were separated by SDS-PAGE and blotted onto a nitrocellulose membrane (Invitrogen). Blots were probed for IκB, phospho-IκB, tubulin, phospho-p38, total p38, phospho-JNK and total JNK (Cell Signaling), phospho-ERK and total ERK (Santa Cruz).

mRNA analysis

BMDM were treated for 2, 4, or 6 hours with TNF and zVAD. Total RNA was isolated using RNeasy mini kit (Qiagen). cDNA was generated using Taqman reverse transcription reagents (Invitrogen) and gene expression was evaluated with the Taqman PCR core reagent kit (Invitrogen) using the commercially available KC primer/probe set (Invitrogen, Mm 04207460_m1). Data were normalized to 18S rRNA.

Phospho-RIP1 ELISA

Phospho-RIP1 ELISAs were performed on lysates produced from TNF (20ng/ml) or TNF + zVAD (20μM, R&D Systems) stimulated TM using MULTI-ARRAY ® 96-well small spot plates (Meso-Scale Discovery) coated with anti-human RIP1 antibody (Abcam). Lysate samples were incubated, and phospho-RIP1 was detected with a novel rabbit anti-RIP1pS166 antibody (manuscript in preparation) and an anti-rabbit IgG, SULFO-tagged detection antibody (Meso-Scale Discovery). Plates were read on a Sector6000 and ECL counts were converted to ng using the standard curve.

Histology

Tissues for histologic examination were collected, immersion fixed, trimmed, decalcified (where applicable) until judged complete by palpation, and processed. Following fixation, tissue samples were embedded in paraffin wax, sectioned, stained with hematoxylin and eosin and examined by light microscopy.

In vitro analysis of cell death

Necroptotic and apoptotic cell death were induced with TNF (50ng/ml BMDM and 10ng/ml TM) and zVAD (50uM BMDM and 20uM TM) and TNF (50ng/ml) and cycloheximide (CHX; 12μg/ml, Sigma) treatment respectively. Cell death evaluation was performed 21 hours post stimulation by quantifying intracellular ATP levels using CellTiter-Glo Viability assay (Promega). Percent survival was calculated for each treatment (TNF treated cells were set to 100% survival). For Caspase 3/7 activity, cells were treated with TNF and CHX for 6 hours. Activity was measured using Caspase-Glo 3/7 assay (Promega). Data were normalized for protein levels. Supernatants were collected for cytokine analysis.

In vivo TNF shock

Mice were injected i.v. with 1.25mg/kg TNF (Cell Sciences) and 16.7mg/kg zVAD (Bachem). Temperature was monitored at regular intervals using a rectal probe. Mice were euthanized once a 7°C temperature loss from baseline was detected, in accordance with our IACUC protocol.

Cpdm mouse analysis

Cpdm mice and crosses were monitored by our veterinary staff and euthanized when the dermatitis was considered to be severe (covering ≥ 50% of the abdomen). Tissues were collected for histopathology.

Statistics

In vitro data are shown as mean +/− standard deviation. *In vivo* data are shown as mean +/− standard error of the mean and were analyzed using a one way ANOVA followed by Bonferroni's post-hoc analysis. *Cpdm* dermatitis data were analyzed by Log-rank (Mantel-Cox) test. * represents a p-value of ≤ 0.05.

Results and Discussion

RIP1 kinase dead mice are viable and healthy

To study the role of RIP1 kinase activity in TNF signaling, we generated a kinase-dead knock-in (*Ripk1*^{K45A}) mouse with a point mutation in the catalytic lysine (K45A) in exon 3 of the *Ripk1* gene (Fig. 1A). *Ripk1*^{K45A} mice were viable and born at the expected Mendelian ratios from interbreeding of heterozygous mice, and displayed normal litter sizes from homozygous breeding paradigms (data not shown). A similar RIP1 kinase-dead mouse with a D138N mutation was published while this manuscript was under review and was also shown to be viable and have a similar phenotype to our *Ripk1*^{K45A} mice (10). This is in contrast to mice lacking RIP1 protein (RIP1 KO) that die one to three days after birth (6). We confirmed the previously reported RIP1 KO phenotype, as exon 3 of our *Ripk1*^{K45A} construct was flanked by *loxP* sites (Fig. 1A), and no RIP1 KO homozygous mice were observed at weaning when knocking out the gene by crossing to a Cre/*loxP*-deleter transgenic line (data not shown).

To confirm that *Ripk1*^{K45A} mice lacked kinase activity we used a newly generated antibody recognizing an autophosphorylation site on RIP1 (manuscript in preparation). Phospho-ELISA analysis detected RIP1 autophosphorylation in response to TNF and zVAD stimulation of cells from *wt* but not *Ripk1*^{K45A} littermate controls (Fig. 1B). Despite lacking kinase activity, protein expression of RIP1, and its necroptosis inducing partner RIP3 (11), were normal in multiple tissues and cell types including spleen, thymus, lymph nodes and macrophages (Fig. 1C and data not shown). A thorough histopathological analysis was undertaken to explore if absence of kinase activity led to any pathologies despite the mice appearing grossly normal. *Ripk1*^{K45A} mice were histologically indistinguishable from wild-type mice in any of the 20 tissues examined (Fig. 1D). This included organs where pathologies were observed in RIP1 KO mice when they were originally described (6). Additionally, no differences were observed in thymic double positive T cell populations

between wild-type and *Ripk1*$^{K45A\ mice}$ (Supplemental Fig. 1). This contrasts to the defect in this population that was seen in RIP1 KO mice (6). By demonstrating that *Ripk1*^{K45A} mice lacking RIP1 kinase activity are viable and healthy, we can attribute the perinatal lethality of the RIP1 deficient mice to an absence of RIP1 scaffolding function.

Ripk1^{K45A} macrophages are selectively protected from TNF-induced necroptosis

We next set out to address which pathways downstream of TNFR1 were affected by the lack of RIP1 kinase activity *in vitro*. To this end, bone marrow derived (BMDM) and thioglycolate elicited macrophages (TM) were isolated from *Ripk1*^{K45A} mice or *wt* littermate controls and stimulated with TNF and the caspase inhibitor zVAD to induce necroptosis. *Ripk1*^{K45A} macrophages were completely protected from undergoing this form of cell death (Fig. 2A). In addition to being protected from cell death, *Ripk1*^{K45A} macrophages showed diminished production of the chemokine KC as compared to *wt* controls (Fig. 2B), consistent with an emerging role for RIP1 kinase activity in the generation of inflammatory cytokines (12). Further investigation revealed that this RIP1-dependent cytokine production was likely to be regulated at the mRNA level, as wild-type mice showed roughly 2-fold higher levels of KC mRNA at 2 hours post stimulation, which preceded RIP1-dependence at the protein level which was not seen until 4 hours post stimulation (Fig. 2C).

We next examined the effect of the absence of RIP1 kinase activity on TNF stimulation of the NFκB pathway and apoptosis. TNF stimulation resulted in an equal pro-survival signal (Fig. 2D) and cytokine production (Fig. 2E) in both the *Ripk1*^{K45A} and *wt* control macrophages. Similarly, *Ripk1*^{K45A} and *wt* control cells were equally susceptible to TNF and cycloheximide (CHX) induced apoptosis (Fig. 2D) and KC production (Fig. 2E). This lack of an effect on TNF-alone signaling was confirmed by examining TNF-driven IκB phosphorylation and degradation (Supplemental Fig. 2A) and p38, JNK or ERK activation out to 2 hours post TNF challenge (Supplemental Fig. 2B and data not shown). Similarly TNF and CHX induced caspase 3/7 activation was also unchanged (Supplemental Fig. 2C). Together, these results show that cells from the *Ripk1*^{K45A} mice are selectively protected against RIP1 kinase-dependent cell death and signaling, in agreement with experiments using the RIP1 inhibitor Nec-1, as well as RIP3 deficient cells (5,13).

Ripk1^{K45A} mice are protected from TNF and zVAD lethal shock

We next assessed the contribution of kinase activity *in vivo*. Previous work has shown that the administration of TNF and zVAD *in vivo* results in a shock like syndrome characterized by temperature loss, inflammatory cytokine production and death (14). This temperature loss has been shown to be partially rescued by blocking the necroptosis pathway through administration of the RIP1 kinase inhibitor Nec-1 or absence of the RIP3 protein (14). To follow up on these observations, TNF and zVAD were dosed to *Ripk1*^{K45A} or *wt* control mice. *wt* mice lost 7°C on average three hours post injection, whereas *Ripk1*^{K45A} mice were nearly completely resistant to the challenge, losing less than 1°C 3 hours post injection (Fig. 3), and surviving to termination of the study at 24 hours post challenge with no signs of morbidity (data not shown). The near complete protection from temperature loss in *Ripk1*^{K45A} mice contrasts with only a partial protection in mice treated with Nec-1. This may be best explained by incomplete blockade of RIP1 kinase activity with Nec-1, as

compounds with better potency and pharmacokinetics can completely block TNF and zVAD induced temperature loss (manuscript in preparation). Additionally, this discrepancy in the level of protection between the *Ripk1*^{K45A} and RIP3 KO mice suggest that RIP1 kinase-dependent, RIP3-independent mechanisms may be involved in driving pathology in the model.

Ripk1^{K45A} × cpdm cross is completely protected from inflammation

We next crossed the *cpdm* strain to the *Ripk1*^{K45A} mice to understand the involvement of RIP1 kinase activity in driving the *cpdm* inflammatory phenotypes. *cpdm* mice develop a severe dermatitis beginning at 6-8 weeks of age (Fig. 4A). *Ripk1*^{K45A} heterozygous SHARPIN-deficient mice showed a small, but significant delay in the onset of the severe dermatitis (Fig. 4B). Remarkably, cross of the *cpdm* to a *Ripk1*^{K45A} homozygous background resulted in a complete protection from the dermatitis phenotype (Fig. 4A and B). In addition to the dermatitis, histopathological examination of the *cpdm* mice showed prominent inflammation in multiple tissues including skin, joint spaces, lung and liver (Fig. 4C). Histopathology changes consisted chiefly of multifocal to diffuse areas of inflammatory cell infiltration and edema, and localized epidermal ulceration and/or epidermal keratinocyte degeneration in the skin and inflammation of synovial membranes along with hyperplasia of the synovial epithelium in the joints (Fig. 4C). Additionally, lung inflammation was associated with interstitial peribronchiolar/peribronchial and perivascular areas, while multifocal inflammation with or without fibrosis was observed in the liver (Fig. 4C). Absence of RIP1 kinase activity protected against all *cpdm*-related inflammatory phenotypes at the histopathological level, with tissues being indistinguishable to those from non-*cpdm* mice (Fig. 4C). Furthermore, *cpdm* mice also display an increase in serum IgM levels compared to wild-type littermate controls that is completely reversed in the *Ripk1*^{K45A} homozygous *cpdm* mice (Fig. 4D).

Given the selective protection of cells from *Ripk1*^{K45A} mice to TNF-induced necroptosis, this makes the complete rescue observed in the *cpdm* × *Ripk1*^{K45A} mice that are sensitive to both TNF-mediated necroptosis and apoptosis surprising. This may highlight the potent inflammatory nature of necroptotic cell death, or alternatively, these results are consistent with emerging data suggesting that RIP1 kinase activity can also drive an apoptotic response under certain conditions (15). Together, these results show that the inflammatory phenotype of the *cpdm* mice is entirely RIP1 kinase-dependent. The absence of another LUBAC family member, HOIL, has been shown to cause autoinflammation and immunodeficiency in humans (16). Although these patients do not develop dermatitis, in some cases the inflammation was completely TNF-dependent (16). This makes it tempting to speculate that similarly to the SHARPIN-deficient mouse, many of the pathologies observed in HOIL-deficient patients are driven by aberrant RIP1 kinase activity.

The data in this paper highlight the utility of the *Ripk1*^{K45A} mice as a tool to dissect the role of RIP1-dependent necroptosis and signaling in mediating inflammation driven by TNF and other factors that stimulate the RIP1 kinase pathway. Our data showing that RIP1 kinase activity completely rescues inflammation in the *cpdm* mouse add to the growing body of evidence that RIP1 kinase-dependent cell death and signaling is highly inflammatory (17).

These data, coupled with the lack of pathology in the absence of RIP1 kinase signaling, makes RIP1 kinase an attractive target for the treatment of complex inflammatory diseases.

Supplementary Material

Refer to Web version on PubMed Central for supplementary material.

Acknowledgments

We thank Drs. Amber Anderson and David Cooper for help with statistical analyses, Angela Dykon and Dr. Sean Maguire for help with animal care and Jon Renninger for his help in coordinating the histopathology.

Supported by N.I.H (PHS grants R01 AI20211 to E.S.M and DP1 OD012198 to W.J.K.).

Abbreviations used in the article

BMDM	bone marrow derived macrophage
CHX	cycloheximide
Cpdm	chronic proliferative dermatitis
CTG	CellTiter-Glo
KO	knockout
LUBAC	linear ubiquitin chain assembly complex
Nec-1	Necrostatin-1
RIP1	receptor interacting protein 1; RIP1
TM	thioglycolate elicited macrophage
TNFR	TNF receptor
wt	wild-type

References

1. Carswell EA, Old LJ, Kassel RL, Green S, Fiore N, Williamson B. An endotoxin-induced serum factor that causes necrosis of tumors. Proc. Natl. Acad. Sci. U. S. A. 1975; 72:3666–3670. [PubMed: 1103152]
2. Aggarwal BB, Gupta SC, Kim JH. Historical perspectives on tumor necrosis factor and its superfamily: 25 years later, a golden journey. Blood. 2012; 119:651–665. [PubMed: 22053109]
3. Festjens N, Vanden Berghe T, Cornelis S, Vandenabeele P. RIP1, a kinase on the crossroads of a cell's decision to live or die. Cell Death. Differ. 2007; 14:400–410. [PubMed: 17301840]
4. Vandenabeele P, Declercq W, Van HF, Vanden Berghe T. The role of the kinases RIP1 and RIP3 in TNF-induced necrosis. Sci. Signal. 2010; 3:re4. [PubMed: 20354226]
5. Degterev A, Hitomi J, Germscheid M, Ch'en IL, Korkina O, Teng X, Abbott D, Cuny GD, Yuan C, Wagner G, Hedrick SM, Gerber SA, Lugovskoy A, Yuan J. Identification of RIP1 kinase as a specific cellular target of necrostatins. Nat. Chem. Biol. 2008; 4:313–321. [PubMed: 18408713]
6. Kelliher MA, Grimm S, Ishida Y, Kuo F, Stanger BZ, Leder P. The death domain kinase RIP mediates the TNF-induced NF-kappaB signal. Immunity. 1998; 8:297–303. [PubMed: 9529147]
7. Emmerich CH, Schmukle AC, Walczak H. The Emerging Role of Linear Ubiquitination in Cell Signaling. Sci. Signal. 2011; 4:re5. [PubMed: 22375051]

8. Gerlach B, Cordier SM, Schmukle AC, Emmerich CH, Rieser E, Haas TL, Webb AI, Rickard JA, Anderton H, Wong WW, Nachbur U, Gangoda L, Warnken U, Purcell AW, Silke J, Walczak H. Linear ubiquitination prevents inflammation and regulates immune signalling. Nature. 2011; 471:591–596. [PubMed: 21455173]

9. HogenEsch H, Gijbels M, Offerman E, van Hooft J, van Bekkum D, Zurcher C. A spontaneous mutation characterized by chronic proliferative dermatitis in C57BL mice. Am J Pathol. 1993; 143:972–982. [PubMed: 8362989]

10. Newton K, Dugger DL, Wickliffe KE, Kapoor N, de Almagro MC, Vucic D, Komuves L, Ferrando RE, French DM, Webster J, Roose-Girma M, Warming S, Dixit VM. Activity of protein kinase RIPK3 determines whether cells die by necroptosis or apoptosis. Science. 2014; 343:1357–1360. [PubMed: 24557836]

11. Chan FK, Baehrecke EH. RIP3 finds partners in crime. Cell. 2012; 148:17–18. [PubMed: 22265396]

12. Christofferson DE, Li Y, Hitomi J, Zhou W, Upperman C, Zhu H, Gerber SA, Gygi S, Yuan J. A novel role for RIP1 kinase in mediating TNF[alpha] production. Cell Death Dis. 2012; 3:e320. [PubMed: 22695613]

13. He S, Wang L, Miao L, Wang T, Du F, Zhao L, Wang X. Receptor interacting protein kinase-3 determines cellular necrotic response to TNF-alpha. Cell. 2009; 137:1100–1111. [PubMed: 19524512]

14. Duprez L, Takahashi N, Van HF, Vandendriessche B, Goossens V, Vanden Berghe T, Declercq W, Libert C, Cauwels A, Vandenabeele P. RIP kinase-dependent necrosis drives lethal systemic inflammatory response syndrome. Immunity. 2011; 35:908–918. [PubMed: 22195746]

15. Abhari BA, Cristofanon S, Kappler R, von SD, Humphreys R, Fulda S. RIP1 is required for IAP inhibitor-mediated sensitization for TRAIL-induced apoptosis via a RIP1/FADD/caspase-8 cell death complex. Oncogene. 2012

16. Boisson B, Laplantine E, Prando C, Giliani S, Israelsson E, Xu Z, Abhyankar A, Israel L, Trevejo-Nunez G, Bogunovic D, Cepika AM, MacDuff D, Chrabieh M, Hubeau M, Bajolle F, Debre M, Mazzolari E, Vairo D, Agou F, Virgin HW, Bossuyt X, Rambaud C, Facchetti F, Bonnet D, Quartier P, Fournet JC, Pascual V, Chaussabel D, Notarangelo LD, Puel A, Israel A, Casanova JL, Picard C. Immunodeficiency, autoinflammation and amylopectinosis in humans with inherited HOIL-1 and LUBAC deficiency. Nat Immunol. 2012; 13:1178–1186. [PubMed: 23104095]

17. Welz PS, Wullaert A, Vlantis K, Kondylis V, Fernandez-Majada V, Ermolaeva M, Kirsch P, Sterner-Kock A, van LG, Pasparakis M. FADD prevents RIP3-mediated epithelial cell necrosis and chronic intestinal inflammation. Nature. 2011; 477:330–334. [PubMed: 21804564]

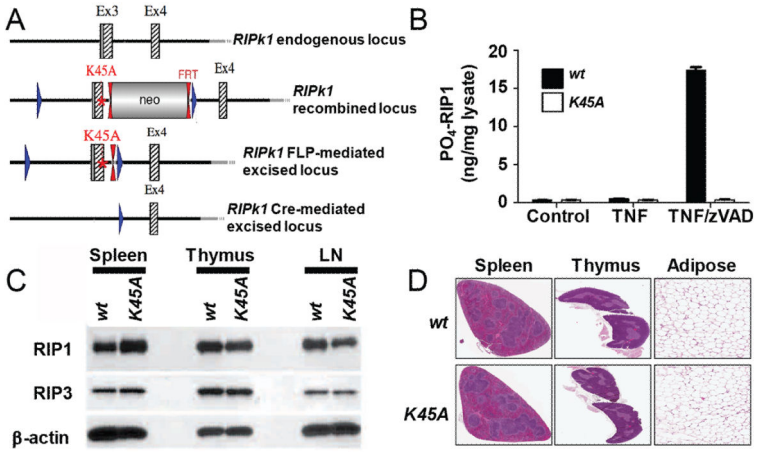

Figure 1.

Ripk1^{K45A} mice are viable and lack pathology associated with the RIP1 KO mouse. (**A**) The *Ripk1* gene-targeting vector was constructed from genomic C57Bl/6 mouse DNA. The K45A point mutation was inserted into *Ripk1* exon 3 while a Neo cassette was inserted in intron 3 flanked by FRT sites for Flp-mediated excision. Exon 3 was flanked by *lox*P sites enabling access to its deletion through Cre-action. (**B**) Phospho-RIP1 ELISA analysis. Lysates were prepared from *wt* (black bars) or *Ripk1*^{K45A} (white bars) macrophages (control), or cells stimulated with TNF or TNF and zVAD for 3 hours. Results are representative of two experiments. (**C**) Western blot analyses of RIP1 and RIP3 expression in the spleen, thymus, and lymph nodes (LN) from *wt* and *Ripk1*^{K45A} mice. β-Actin is shown as a loading control. Data are representative of three experiments. (**D**) Histopathology analysis of spleen, thymus and white adipose tissue from 10 to 12 week old *wt* littermate and *Ripk1*^{K45A} mice. Data are representative of three *wt* and 5 *Ripk1*^{K45A} mice.

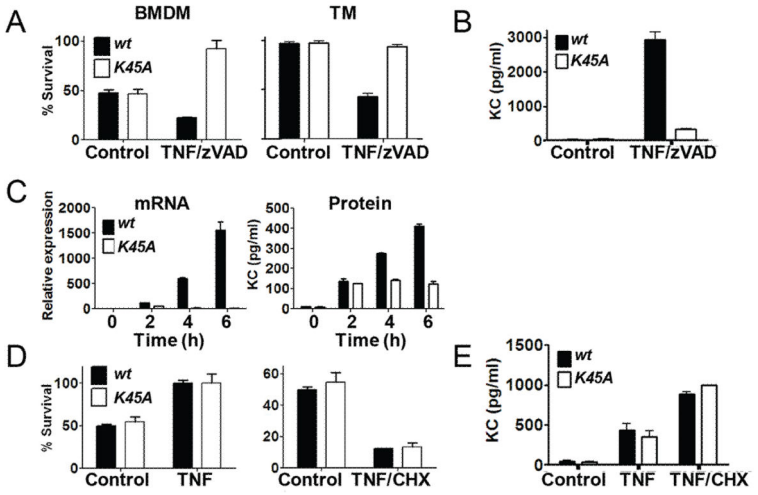

Figure 2.

Macrophages from *Ripk1*^{K45A} mice are protected from necroptosis, but not NFκB activation or apoptosis *in vitro*. (**A**) CTG viability analysis of BMDM or TM from *wt* (black bars) or *Ripk1*^{K45A} (white bars) mice. Macrophages were left untreated (control) or stimulated with TNF and zVAD. (**B**) Measurement of KC release from BMDM treated as in (A). (**C**) KC mRNA and protein analysis from BMDM from *wt* or *Ripk1*^{K45A} mice treated with TNF and zVAD for the indicated times (**D**) CTG viability analysis of BMDM from *wt* (black bars) or *Ripk1*^{K45A} (white bars) mice. Macrophages were either left untreated (control) or stimulated with TNF or TNF and CHX for 21 hours. (**E**) Measurement of KC release from BMDM treated as in (D).

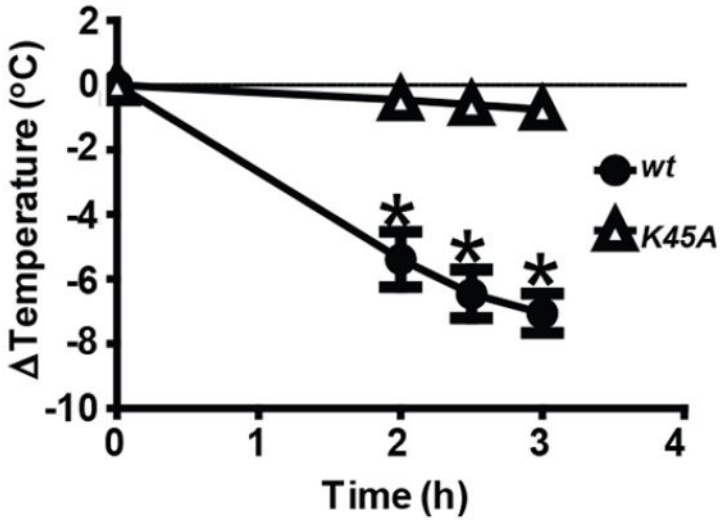

Figure 3.

Ripk1^{K45A} mice are protected from TNF and zVAD-induced shock. *wt* (closed circles) or *Ripk1*^{K45A} (open triangles) mice were injected with TNF and zVAD. Temperature was monitored over three hours, and animals were euthanized after a 7°C loss. Data are representative of at least 3 experiments, each containing seven mice per group.

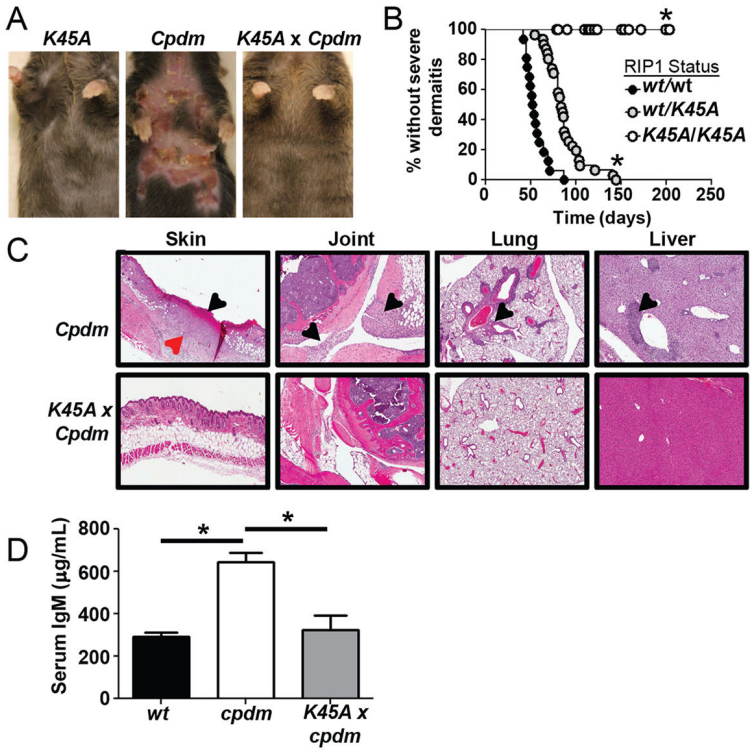

Figure 4.

RIP1 kinase activity drives inflammation in *cpdm* mice. (**A**) Representative photo of *Ripk1*^{K45A}, *cpdm* and *Ripk1*^{K45A} × *cpdm* mice at 7-8 weeks of age. (**B**) *Cpdm* and *Ripk1*^{K45A} heterozygous mice were interbred to produce *cpdm* mice that were *wt* (WT/WT, black circles), heterozygous (WT/K45A, grey circles) or homozygous (K45A/K45A, white circles) for the *Ripk1*^{K45A} gene. Dermatitis was considered to be severe (covering ≥ 50% of the abdomen). * indicates significantly different from RIP1 WT/WT (black circles) group. (**C**) Representative histology from *cpdm* or *Ripk1*^{K45A} × *cpdm* mice at 7-8 weeks of age. Arrowheads in each panel point to, respectively, epidermal ulceration (black arrowhead) and dermal inflammation (red arrowhead) in skin, regions of inflammation in joint, regions of inflammation in lung and areas of inflammation in the liver. (**D**) Analysis of serum IgM levels.